

Description of a Neotropical gall inducer on Araceae: *Arastichus*, gen. nov. (Hymenoptera, Eulophidae) and two new species

Y. Miles Zhang¹, Michael W. Gates¹, Paul E. Hanson², Sergio Jansen-González^{2,3,4}

1 Systematic Entomology Laboratory, Agricultural Research Service, U.S. Department of Agriculture, c/o National Museum of Natural History, Smithsonian Institution, P.O. Box 37012, MRC-168, Washington, DC 20013-7012, USA **2** Escuela de Biología and Centro de Investigación en Biodiversidad y Ecología Tropical (CIBET), Universidad de Costa Rica, A.P. 11501-2060, San Pedro de Montes de Oca, San José, Costa Rica **3** Universidad Nacional, Centro Mesoamericano de Desarrollo Sostenible del Trópico Seco, Nicoya, Guanacaste, Costa Rica **4** Avenida Bandeirantes, 3900, CEP 14040-901, Pós-Graduação em Entomologia – Bloco 9, FFCLRP, USP, Ribeirao Preto, SP, Brazil

Corresponding author: Michael W. Gates (Michael.Gates@usda.gov)

Academic editor: Petr Janšta | Received 4 May 2022 | Accepted 14 July 2022 | Published 31 August 2022

<https://zoobank.org/3E9AD341-8B60-47AF-A14B-F8F2D885174B>

Citation: Zhang YM, Gates MW, Hanson PE, Jansen-González S (2022) Description of a Neotropical gall inducer on Araceae: *Arastichus*, gen. nov. (Hymenoptera, Eulophidae) and two new species. Journal of Hymenoptera Research 92: 145–172. <https://doi.org/10.3897/jhr.92.85967>

Abstract

A new genus of a Neotropical gall inducing tetrastichine eulophid on Araceae is described and confirmed using Ultraconserved Elements (UCE) phylogenomic data. *Arastichus* Gates, Hanson, Jansen-González & Zhang, **gen. nov.**, includes two new species and one species transferred from *Aprostocetus* Westwood: *A. capipunctata* Gates, Hanson, Jansen-González & Zhang, **sp. nov.**, *A. gallicola* (Ferrière), **comb. nov.**, and *A. gibbermau*, Gates, Hanson, Jansen-González & Zhang, **sp. nov.**

Keywords

Chalcidoidea, *Philodendron*, Phytophagy, Tetrastichinae, *Thaumatococcus*

Introduction

The Chalcidoidea is a large and diverse superfamily with broad biological diversity (Heraty et al. 2013), and with estimates of over 500,000 species (Noyes 2019) on Earth. Although primarily entomophagous, many phytophagous forms are known, among these the gall inducers that deform plant tissue in order to complete their development. The biology of gall inducers and the evolution of gall induction in Chalcidoidea have been reviewed recently (LaSalle 2005). Gall induction has evolved in seven different families of Chalcidoidea, with at least 16 independent origins both from entomophagous and phytophagous ancestors (LaSalle 2005; Böhmová et al. 2022). This includes the Eulophidae, the largest and most diverse chalcidoid family including over 4,300 species in 332 genera (Noyes 2019; Rasplus et al. 2020). The diversity of gall inducing eulophids is highest in the Australian Opheliminae and the cosmopolitan Tetrastichinae, the latter is a large and diverse subfamily with 15 genera recorded as phytophagous species (Kim et al. 2004, 2005; Mendel et al. 2004; LaSalle 2005; Kim and LaSalle 2008; Rasplus et al. 2011; Fisher et al. 2014). Overall, knowledge of the specific biology of gall associated tetrastichines is minimal but falls into three categories: parasitoid of gall inducer, inquiline, or gall inducer. LaSalle (2005) divides gall-associated tetrastichines into two groups: (1) the Australian inducers that gall Myrtaceae, and (2) mostly Neotropical groups that are often larger and more heavily sclerotized.

LaSalle (1994) records seven plant families serving as hosts for gall inducing Tetrastichinae: Araceae, Chenopodiaceae, Euphorbiaceae, Fabaceae, Myrtaceae, Myrsinaceae, and Solanaceae. Additionally, tetrastichines have also been recorded as gall inducers from Casuarinaceae (Fisher et al. 2014), Sapotaceae (Singh et al. 2022), and Smilacaceae (Gates et al. 2020). In evaluating the gall-inducers associated with the Araceae (Alismatales) in general, focusing specifically on Hymenoptera, we note that very few taxa are known to be associated with this family, particularly as suspected phytophages (Table 1).

Here we describe a new genus of Neotropical tetrastichines inducing galls on *Thaumatococcus* and *Philodendron* (Araceae), *Arastichus* Gates, Hanson, Jansen-González & Zhang, gen. nov. (Fig. 1). We describe two new species: *A. capipunctata* Gates, Hanson, Jansen-González & Zhang, sp. nov., and *A. gibernau*, Gates, Hanson, Jansen-González & Zhang, sp. nov. Additionally, we transfer *Trichaporus gallicola* Ferrière to *Arastichus*, comb. nov., from its current placement in *Aprostocetus* Westwood, and provide a redescription along with designation of lectotype.

Materials and methods

Collection and identification

Mature infrutescences of *Thaumatococcus bipinnatifidum* and *Philodendron radiatum* were cut from the plant in the laboratory, or mass reared in bags hung on clothes-

Table 1. Hymenoptera associated with Araceae.

Family (Subfamily)	Species	Plant	Reference
Eulophidae (Tetrastichinae)	<i>Arastichus gallicola</i> (Ferrière)	<i>Philodendron</i> sp. Schott	DeSantis 1979
		<i>P. undulatum</i> Engler	Ferrière 1924
		<i>P. tweedieanum</i> Schott (as <i>P. dubium</i> (Chodat and Vischer))	This study
		<i>Thaumatophyllum bipinnatifidum</i> (Schott ex Endl.) (as <i>P. petraeum</i> Chodat and Vischer)	
		<i>T. solimoense</i> (A.C.Sm.) Sakur., Calazans & Mayo	
Eulophidae (Tetrastichinae)	<i>Arastichus capipunctata</i> sp. n.	<i>Philodendron radiatum</i> (Schott)	This study
Eulophidae (Tetrastichinae)	<i>Arastichus gibernau</i> sp. n.	<i>Philodendron hederaceum</i> var. <i>oxycardium</i> Schott	This study
Eulophidae (Entedoninae)	<i>Ametallon deanthurium</i> Hansson	<i>Anthurium cuspidatum</i> Mast.	Hansson 2004
Eurytomidae (Eurytominae)	<i>Prodecatoma philodendri</i> Ferrière	<i>Philodendron</i> sp.	DeSantis 1979
		<i>Philodendron hederaceum</i> (Jacq.) (as <i>P. oxycardium</i> (Schott))	DeSantis 1980
		<i>P. tweedieanum</i> (as <i>P. dubium</i>)	DeSantis and Fidalgo 1994
			Ferrière 1924
			Gibernau 2002
	<i>T. solimoense</i> (A. C. Sm.) (as <i>P. solimoense</i>)	Lotfalizadeh et al. 2007	
		Perioto and Lara 2019	
Eurytomidae (Eurytominae)	<i>Aranedra mills</i> Burks	<i>Philodendron</i> sp.	Burks 1971
			DeSantis 1979
Braconidae (Doryctinae)	<i>Monitoriella elongata</i> Hedqvist	<i>P. radiatum</i>	Infante et al. 1995
			Shimbori et al. 2011

line. As the spathe was still closed in most of the infrutescences, careful incisions with a knife were used to expose the fruits beneath. A few fruits were dissected under a stereomicroscope to ensure they had galls with pupae or adults inside. The selected infrutescences were then put in individual organdy bags (40 cm × 30 cm) for wasp emergence. Emerging wasps were collected and stored in 70% EtOH.

Ethanol-preserved specimens were dehydrated through increasing concentrations of ethanol and transferred to hexamethyldisilazane (HMDS) (Heraty and Hawks 1998) before point-mounting. A Nikon SMZ1500 stereomicroscope with 10× oculars (Nikon C-W10X/22) and a Chiu Technical Corporation Lumina 1 FO-150 fiber optic light source were used for point-mounted specimen observation. Mylar film was placed over the ends of the light source to reduce glare from the specimen. Scanning electron microscope (SEM) images were taken with a Hitachi TM3000 (Tungsten source). Body parts of a disarticulated specimen were affixed to 0.1 mm minuten pins with Loctite Ultra Gel super glue. These were then adhered to a 12.7×3.2 mm Leica/Cambridge aluminum SEM stub by a carbon adhesive tab (Electron Microscopy Sciences, #77825-12). Stub-mounted specimens were sputter coated with gold-palladium using a Cressington Scientific 108 Auto from at least three different angles to ensure complete coverage (~20–30nm coating). One set of wings was removed and slide-mounted in polyvinyl alcohol prior to imaging; wings were photographed with a Olympus SC-100 digital camera attached to a Olympus BX43 light microscope and processed using

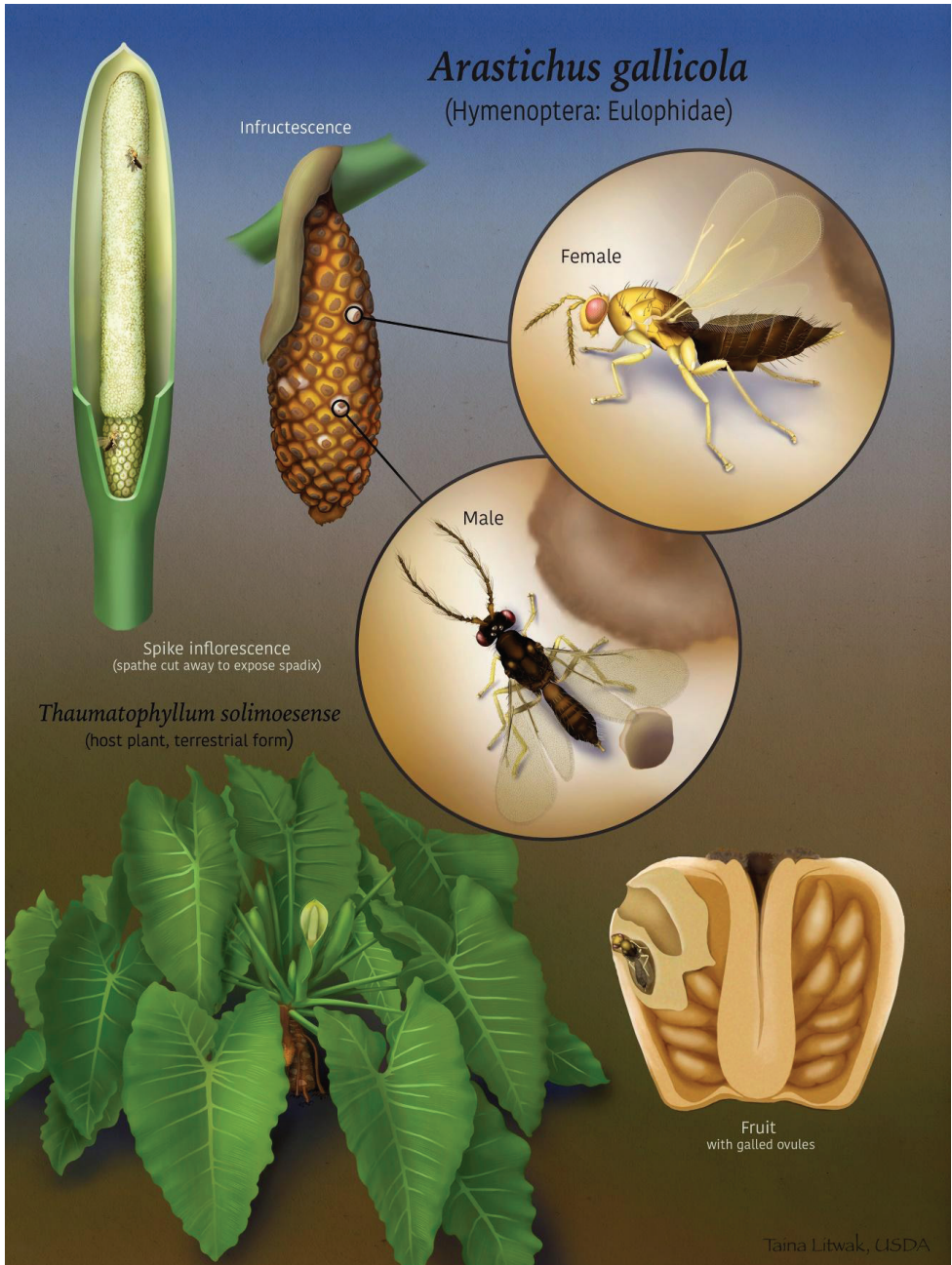


Figure 1. Illustration of the lifecycle of *Arastichus gallicola* with its host plant, *Thaumatophyllum solimoense* (Arecaceae). Illustrated by Taina Litwak.

analySIS getIT 5.2 (Olympus Soft Imaging Solutions). The habitus image was captured using an EntoVision Imaging Suite, which includes a firewire JVC KY-75 3CCD digital camera mounted on a Leica M16 zoom lens via a Leica z-step microscope stand.

The program Cartograph 5.6.0 (Microvision Instruments, France) was used to merge an image series into a single in-focus, composite image. Lighting was achieved using techniques summarized in Buffington et al. (2005), Kerr et al. (2008), and Buffington and Gates (2008). When possible, male and female genitalia were extracted, cleared with KOH 10% and temporarily mounted in glycerin for imaging. Genitalia were photographed using the same setup as for wings (indicated above). These and SEM images were used for the elaboration of schemes of each genitalia using GIMP 2.8.10.

Morphological terminology follows Gibson (1997), while the surface sculpture follows Harris (1979). Several measurements were taken, including: body length, in lateral view from the anterior projection of the face to the tip of the metasoma; head width through an imaginary line connecting the farthest lateral projection of the eyes; head height through an imaginary line from the vertex to the clypeal margin bisecting both the median ocellus and the distance between the toruli; malar space, in lateral view between the ventral margin of the eye and lateral margin of the oral fossa; eye height in anterior view; vertex bristle in anterior view; mesoscutum and scutellum, in dorsal view through imaginary, median transverse and longitudinal lines; marginal vein, the length coincident with the leading fore wing edge to the base of the stigmal vein; stigmal vein, the length between its base on the marginal vein (M) and its apex; postmarginal vein (PMV), the length from the base of the stigmal vein (S) to its apex on the leading fore wing edge. Metasomal sclerites were measured dorsally along the midline. Abbreviations used: **A1–n** (anellus), **F1–n** (funicular segment), **LOL** (lateral ocellar line), **OOL** (ocellocular line), **POL** (posterior ocellar line), **SMV** (submarginal vein), **A** (anellus), **C** (clava), **F** (funicle), **MPS** (multiporous mlate sensilla), **Gt_{1–n}** (gastral tergites), **Gs1–n** (gastral sternites). The antennal formula consists of: scape, pedicel, anelli, funiculars, clava.

Specimens are deposited in the following collections: **ANIC** (Australia National Insect Collection, Canberra, Australia), **BMNH** (The Natural History Museum, London, England), **CNCI** (Canadian National Collection, Ottawa, Canada), **CNIN** (National Collection of Insects – The National Autonomous University of Mexico, Mexico City, Mexico), **MNHN** (The National Museum of Natural History, Paris, France), **MZUCR** (Museum of Zoology – University of Costa Rica, San José, Costa Rica), **MZUSP** (Museum of Zoology – University of São Paulo, São Paulo, Brazil), **USNM** (National Museum of Natural History, Smithsonian Institution, Washington, D.C., USA).

Molecular analysis

One specimen each of *A. gallicola* and *A. capipunctata* were extracted, amplified, and sequenced at the Laboratories of Analytical Biology (LAB) at the Smithsonian Institution's National Museum of Natural History (NMNH, Washington, DC, USA). A modified Ultraconserved Elements (UCE) protocol was used (Faircloth et al. 2012; Branstetter et al. 2017) along with the HymV2P probe set to enrich the UCE loci, (Branstetter et al. 2017). The library was sent to Admera Health (South Plainfield, NJ) and sequenced on an Illumina HiSeq 4000 (150-bp paired-end, Illumina Inc., San Diego, CA, USA). Additional eulophid UCE sequences were supplemented from Cruaud et al. (2019) and Rasplus et al. (2020).

PHYLUCE v1.7.0 (Faircloth, 2015) was used for UCE processing. SPAdes v3.14.0 (Bankevich et al. 2012) was used to align the contigs, sequences were aligned using MAFFT v7.490 (Katoh and Toh 2008), and trimmed using Gblocks v0.91b (Castresana 2000) with the following settings: b1 = 0.5, b2 = 0.5, b3 = 12, b4 = 7. A 50% complete matrix was used for downstream phylogenomic analysis. Additionally, fragments of legacy markers (COI, 28S, and CytB) were extracted from the UCE contigs using PHYLUCE. Trimmed reads for the newly generated sequences in this study are available from the National Center for Biotechnology Sequence Read Archive (SRA; BioProject ID PRJNA827143), and Sanger markers are available on GenBank (Suppl. material 1).

Phylogenomic analysis was conducted under the maximum likelihood (ML) criterion with IQ-TREE v2.1.1 (Minh et al. 2020), partitioning based on loci and with the best models of nucleotide substitution selected in ModelFinder with “-m MFP” (Kalyaanamoorthy et al. 2017). To assess nodal support, we performed a Shimodaira-Hasegawa approximate likelihood-rate test (SH-aLRT, Guindon et al. 2010) with 1000 replicates using the “-alrt” flag, and 1000 ultrafast bootstrap replicates (UFBoot2; Hoang et al. 2017) using “-bb”. Only nodes with support values of SH-aLRT ≥ 80 and UFBoot2 ≥ 95 were considered robust.

Results

The 50% UCE matrix consisted of 567 loci, with *A. capipunctata* and *A. gallicola* having 1715 and 1802 UCE loci recovered, respectively. The topology recovered was largely identical to that of Rasplus et al. (2020). The new genus *Arastichus* was recovered within the subfamily Tetrastichinae with strong support (Fig. 2). *Arastichus* is within the *Aprostocetus* group *sensu* Rasplus et al. (2020), and the sister to *Neohyperteles* DeSantis with strong support (Fig. 2).

Arastichus Gates, Hanson, Jansen-González & Zhang, gen. nov.

<https://zoobank.org/6DB405D8-4660-4698-A9B6-1950816E86DF>

Figs 3–25

Type species. *Arastichus gallicola* (Ferrière).

Diagnosis. Vertex with single erect seta mesad to eye margin, $\sim 0.5\times$ eye height (Fig. 10); vertex depressed posteriad and laterad lateral ocelli (Figs 12, 22); toruli positioned above middle of face, $1\text{--}1.5\times$ torular diameters from median ocellus (Figs 10, 21, 24); intrascrobal carina step like in lateral view with V-like carinae diverging to lateral margins of median ocellus (Figs 12, 22); antennal formula 11242 (Fig. 14) or 11342 in *A. capiculata*. A1 $\sim 1.5\times$ wider at apex rather than base (note: often appears subdivided, representing fusion of two segments) wedge-like in lateral view, longest ventrally; ventral plaque present in male scape (Figs 5, 7, 9); clypeus bilobed, lobes apically truncate; gena ventrally extended beyond oral fossa/base of mandible (Figs 10, 21, 24); mesosoma shiny dorsally (Fig. 23); scutellum lacking submedian grooves (Figs 16, 23); petiole

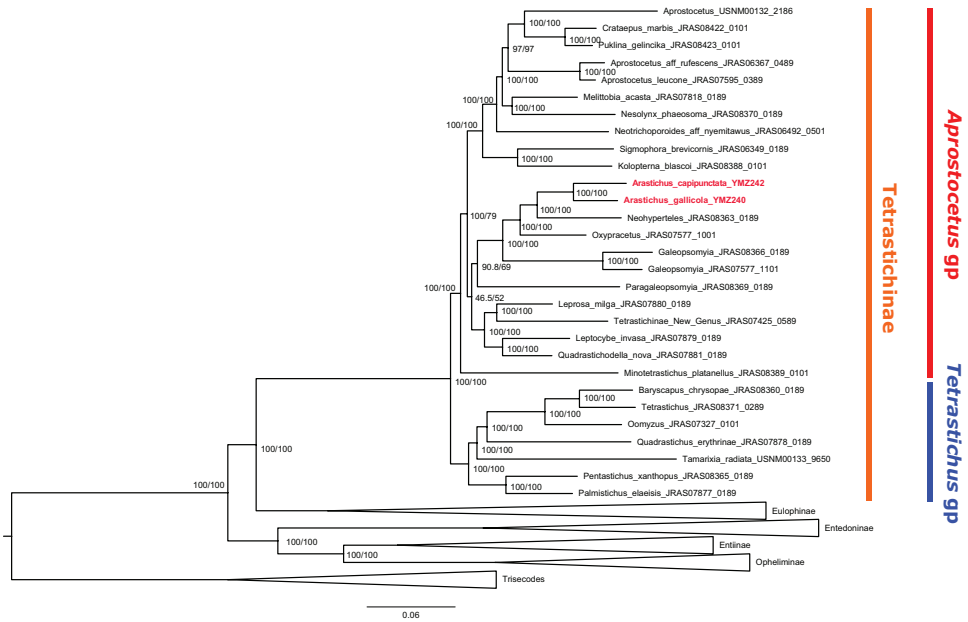


Figure 2. Maximum likelihood reconstruction of Eulophidae phylogeny inferred from 50% complete matrix of 567 Ultraconserved Elements (UCE) loci. Support values shown as SH-aLRT/UFBoot2. All nodes except for Tetrastichinae collapsed, with the two major genus groups (*Aprostocetus* group and *Tetrastichus* group) highlighted, and *Arastichus* in red.

membranous ventrally; a tuft or sometimes one seta(e) anterad mesocoxa (Fig. 9); propodeal spiracles large, $\sim 0.3 \times$ length propodeum; distinct, suberect setation on mesal surface of procoxa and metacoxa (Figs 8, 9), Gt_6 with spiracular rim elevated (Fig. 19).

Arastichus gallicola was first described by Ferrière (1924) as *Trichaporus gallicola*, which was then transferred to *Exurus* Philippi by Costa Lima (1959a). LaSalle (1994) synonymized *Exurus* with *Aprostocetus*, through its type species *E. colliguayae* Philippi. He was hesitant about the status of *A. gallicola* (Fig. 3) as he was not able to examine any type specimens, but commented that it is quite distinct and warranted its own genus. As Ferrière did not designate a holotype, we hereby designate the top left specimen (female) on the pin with three other specimens as the lectotype (Fig. 3). The degree of morphological variation seen in *Aprostocetus* makes it difficult to characterize consistently using few characters; however, according to LaSalle (1994), most species have the SMV with ≥ 3 seta, propodeal spiracle partially covered by overhanging lobe of callus, and one cercal setae distinctly longest and sinuate or curved. Although *Arastichus* shares these diagnostics, several additional apomorphies set it apart from *Aprostocetus* (as noted in the diagnosis above).

Description. Coloration: Female. Length 3.8–5.2 mm. Head, antennae, body, coxae, and legs yellow or brown (Figs 3–9). Tegula pale golden. Pronotum either completely brown, or yellow except for the anterolateral panel. Ventral mouthparts and tarsomeres pale yellow. Female fore wing with soft opaque area at basal and cubital



Figure 3. Dorsal and lateral habitus of *Arastichus gallicola* lectotype (female on the top left), along with three paralectotypes on the same pin.

folds, disc hyaline (Fig. 4). Male fore wing with opaque base of cubital and basal folds; disc with soft opaque pattern (Fig. 5).

Head: Surface rugulose or umbilicately punctate dorsally, laterally, and anteriorly, 1.3–1.6× as broad as high. Supraclypeal area concave, glabrous, asetose (Figs 10, 21, 24), extending to toruli; lower tentorial pits minute. Genal carina present, extending to lower third of eye posteriorly (Figs 10, 13). Torulus with dorsal margin positioned at lower ocular line; intertorular space punctate, obtusely pointed; scrobal depression margined laterally, margin fading dorsally, reticulate with fine irregular rugae and with median carina between depressions in ventral half (Fig. 10). Eyes setose, seta sparsely distributed and very short. Mandible tridentate with apical and middle teeth acute, basal tooth broad and rounded (Fig. 21). Clypeus emarginate in step-like manner (Fig. 21), medially produced. Posterior surface of head without postgenal lamina, postgenal grooves slightly ridged, slightly convergent ventrally, extending to upper margin of hypostomal bridge; dorsal margin of lateral foraminal plate obliterated; subforaminal plate absent; postgenal sulci distinct; postgenal bridge glabrous (Fig. 11). Antenna (Figs 14, 15) with scape broadest medially, coarsely imbricate. Pedicel triangular in



Figure 4–5. Lateral habitus of *Arastichus gallicola* **4** female **5** male.

lateral view, narrowed ventrally; anelli (two in all species except *A. capipunctata*, which has three) transverse, glabrous; F1 chalice-shaped, imbricate in basal half (Fig. 14); funicle with each segment fusiform, longer than broad, apically truncate with two rows

of MPS and sparse, semi-erect setation; F5–6 fused, apex with radially asymmetric sensillar area (Fig. 14).

Mesosoma: Surface smooth, rugulose or umbilicate with interstices alveolate. Pronotum in dorsal view 2.2–3.3× as broad as long. Mesoscutal midlobe 1.0–1.1× as broad as long; notaulus complete, clearly indicated (Fig. 16). Scutellum 1.2–1.3× as long as broad at its widest; broadly convex dorsally. Scutellum distinctly overhanging dorsellum. Sublateral prepectal concavity shallow; epicnemium flattened, with superficial submedial, shallow depressions to receive procoxa, these separated by low carina connecting to epicnemial carina ventrally. Procoxa imbricate anterobasally and medially, flat, low diagonal carina separating this area from umbilicately punctate anteroventral and lateral portion of procoxa; mesocoxa rugulose to imbricate; mesocoxal foramina narrowly open posteriorly; metacoxa rugulose to imbricate. Metapleuron and lateral areas of propodeum shallowly umbilicate, propodeum vaguely rounded laterally (Fig. 20), bordered laterally by reticulate sculpture overlain with umbilicate punctation; spiracle situated about 1/3 its greatest diameter from dorsellum, median channel with series of distinct transverse carinae (Fig. 20). Fore wing hyaline, venation whitish, setae pale brown, evenly distributed; PMV 1.0–1.1× of V and S 0.7–0.8× of M. Basal cell delimited by cubital and basal folds; speculum present; disc uniformly setose; number of dorsal setae on submarginal vein: female: 2–3, male: 1–4. Parastigma not swollen; marginal vein constricted near its base after parastigma and three times as long as stigmal vein. Stigmal vein at an angle of 20°–30° in relation to marginal vein. Uncus small, not extending far from stigma. Postmarginal vein reduced, less than 1/4 of stigmal vein (Figs 4, 5). Hind wing disc evenly setose. with apex of vein (at hamuli) not swollen or knobbed but darkened, with three hamuli.

Metasoma: Petiole 0.3–0.4× as long as broad in dorsal view, laterally protuberant, connected by dorsal transverse carina. Gaster ovate in lateral view; all terga with finely imbricate sculpture, evenly setose, setae fine and erect; Gt₁ depressed behind petiole, setose; Gs1 fused with petiole (Fig. 19); syntergum short, setose; third valvula setose apically, arranged radially and curved.

Genitalia: Female: First valvifer falcate 1/4–1/8 of ovipositor total length, articulates with T9 and the second valvifer very near each other, on its proximal end; second valvifer broad, sickle-shaped; second valvula 3/4 of ovipositor length, with row of 3–4 spaced setae at apical half; third valvula 1/3–1/5 of total ovipositor length (Fig. 26). **Male:** Phallobase cylindrical, 1.5–2.0× as long as wide, paramere pointed with one apical seta, 1/5× the length of phallobase. Volsella 1/2–1/3 of paramere length. Digitus dorsoventrally flattened, bean-shaped in either ventral or dorsal view, 2–3× as long as wide, bearing a single apical digital spine. Aedeagus cylindrical, dorsoventrally flattened, pointed or round at apex (Fig. 27).

Etymology. Name from the host plant family, Araceae. Gender masculine.

Biology. Ferrière (1924) first described *Arastichus gallicola* (as *Trichoporus gallicola*) and defined the species as gall inducer on pistilate flowers of *Philodendron selloum* (now a synonym of *Thaumatococcus* (*Philodendron*) *bipinnatifidum* (Mayo 1991) (Fig. 3). Gibernau et al. (2002) described the galls of *A. gallicola* on flowers of *T. solimoense* and reported it as a seed predator. Recently, a more detailed study of the developmental biology of *A. gallicola* discards seed predation and supports the idea that this species is a gall inducer specialized on ovaries of *T. bipinnatifidum* (SJG, unpublished).

Female wasps of *A. gallicola* oviposit during the period of anthesis which lasts 24–48 hours, when the inflorescence spathe is open and leaves the hundreds of pistillate flowers accessible to pollinators and female *Arastichus* (Gibernau et al. 2002). Once anthesis ends the spathe closes and the space between the spathe and the inflorescence fills with a liquid, often trapping and killing the female wasps inside.

Time of development can vary from one to four months in *Arastichus gallicola*. Once the infrutescence attains maturity, the spathe develops an encircling dehiscent line at its base and falls, uncovering the orange fruits and galls. Exposure of galls to light and outer atmosphere might trigger adult wasp emergence from the galls, which is done by chewing through each gall wall. A single wasp develops per gall with up to six galls developing in a single fruit. It is possible to find infrutescences and/or fruits containing only seeds, combinations of seeds and galls, or only galls (Fig. 1).

Although we have detailed information about gall induction only in *A. gallicola*, it is possible that the other two species of *Arastichus* are also gall inducers rather than seed predators. Examination of collected material for *A. gibernau* and *A. capipunctata* indicates that the biology of these species should not be very different from that of *A. gallicola*.

The eurytomid *Prodecatoma philodendri* is associated with the galls of *Arastichus gallicola* and *A. gibernau*. Ferrière (1924) reported that *Prodecatoma* were phytophagous, and oviposits from the outside when the spathe is closed and *Arastichus* galls are in the process of formation (Gibernau et al. 2002; SJG pers. obs.). When examining the cavities from which *Prodecatoma* adults emerge, a series of tunnels communicate with adjacent *Arastichus* galls. These attacked galls contained dismembered body parts of *Arastichus* pupae, indicating that *Prodecatoma* larvae might consume several of them along with some gall tissue (Gibernau et al. 2002; SJG pers. obs.); this is in line with the fact that the adult *Prodecatoma* is about 4–5 times larger than the *Arastichus* adult. Thus, taken all together, *P. philodendri* is likely entomophytophagous, a common mode of feeding within Eurytomidae.

It is difficult to estimate the taxonomic breadth of the relationship between *Arastichus* and Araceae. *Philodendron* is traditionally subdivided in three subgenera: *Meconostigma*, *Philodendron* and *Pteromischum*, but members of *Meconostigma* have been recently recognized as a distinct genus *Thaumatophyllum* Schott (Sakuragui et al. 2018). *Arastichus* has been found in species belonging to *Thaumatophyllum* (*T. bipinnatifidum*, *T. solimoesense*), and in the subgenus *Philodendron* (*P. radiatum*). SJG has collected what seem to be female *Arastichus* body parts from inside closed spathes of *P. cordatum* and *P. curvilobum* in Brazil. Further studies and more extensive collecting are needed to determine the degree of species-specificity and to determine whether *Arastichus* is present in the subgenus *Pteromischum* as well.

Key to Species of *Arastichus*

- 1 Mesoscutum bilobed at posterior margin (Fig. 23). Face with numerous large punctures (Figs 21, 22). Female body (excluding legs and lower face) completely brown (Fig. 6).....***A. capipunctata* sp. nov.**
- Mesoscutum straight or slightly emarginate at posterior margin (Fig. 16). Face with at most a few faint, widely spaced punctures (Figs 10, 24). Female head and thorax extensively yellow (Figs 4, 8).....**2**

- 2 Posterior corner of metapleuron with circular fossa that is at least half as wide as propodeal spiracle (Fig. 25, arrow). Vertexal suture rounded where it curves down along the inner eye margin (Fig. 24).....*A. gibernau* sp. nov.
- Posterior corner of metapleuron without a noticeable fossa, or with an elongate depression (Fig. 4). Vertexal suture angulate or rounded where it reaches the inner eye margin (Fig. 10).....*A. gallicola* (Ferrière)

***Arastichus capipunctata* Gates, Hanson, Jansen-González & Zhang, sp. nov.**

<https://zoobank.org/3F50B966-83A2-456F-9D56-52C800D8C907>

Figs 6, 7, 21–23

Diagnosis. *Arastichus capipunctata* can be distinguished from all other known species through the bilobed mesoscutum at the posterior margin (Fig. 23), and the numerous large punctures on the face (Figs 21, 22). The coloration of both males and females are uniformly brown (Figs 6, 7). Females have three anelli.

Material examined. *Holotype* COSTA RICA • [1F]; Guanacaste 9km S Santa Cecilia, Estación Biológica Pitilla, 600 m 18.XII.2010. L. Chavarria leg.; USNMENT01788075; deposited in USNM. *Paratypes*: [44F, 26M]; same information as holotype; USNMENT01829180–250; USNM. [4F, 4M]; same information as holotype; ANIC. [4F, 4M]; same information as holotype; BMNH. [4F, 4M]; same information as holotype; CNCI. [4F, 4M]; same information as holotype; MNHN. MEXICO • [3F, 4M]; Veracruz, San Andrés Tuxtlas, Est. Biol. Tropical Las Tuxtlas, 2.III.2017, 124 m 18°35'22.1"N, 95°5'24.9"W, G. Amancio, A. Aguirre, F. Ozul leg., ex galled fruit *Philodendron radiatum*; USNMENT01788065–69; USNM. [1F, 1M]; same information as before; CNIN. [46F, 52M]; same information as before; MZUCR.

Description. Holotype female. Body length 2.9 mm. **Color:** Brown except for the following yellow: scape, pedicel, lower face, prepectus, legs (except metacoxa brown), wing veins white to brown (Fig. 6).

Head. 1.45× as broad as high, with large punctures (Figs 21, 22); anterior tentorial pits with epistomal groove extending ventrally. Supraclypeal area glabrous; clypeus bilobed. Lower margin of eyes slightly sunken; malar suture distinct; malar space 0.37× eye height, asetose beneath eye in elongate microreticulate area; frons protuberant. Preorbital carina absent; intrascrobal area divergent dorsally to laterad anterior ocellus, delimiting shallow equilateral triangular depression in front of anterior ocellus. Ratio of LOL:OOL:POL as 1:2.1:2.5. Vertexal seta 0.45× eye height; vertexal suture rounded at inner eye margin (Fig. 21); occipital margin without transverse, sinuate carina. Head posteriorly lacking postgenal lamina, postgena with ventral depression near ventral margin.

Antenna. (Fig. 6) ratio of scape (minus radicle): pedicel: A1: A2: A3: F1: F2: F3: F4: F5: club as 74:14:1:1:2:18:18:18:18:16:16; A1 constricted medially; A2 transverse; one row of MPS on all funicular segments, erect setae at 45° angle to angle to funicular segment, shorter than the funicular segment to which it is attached (Fig. 6).

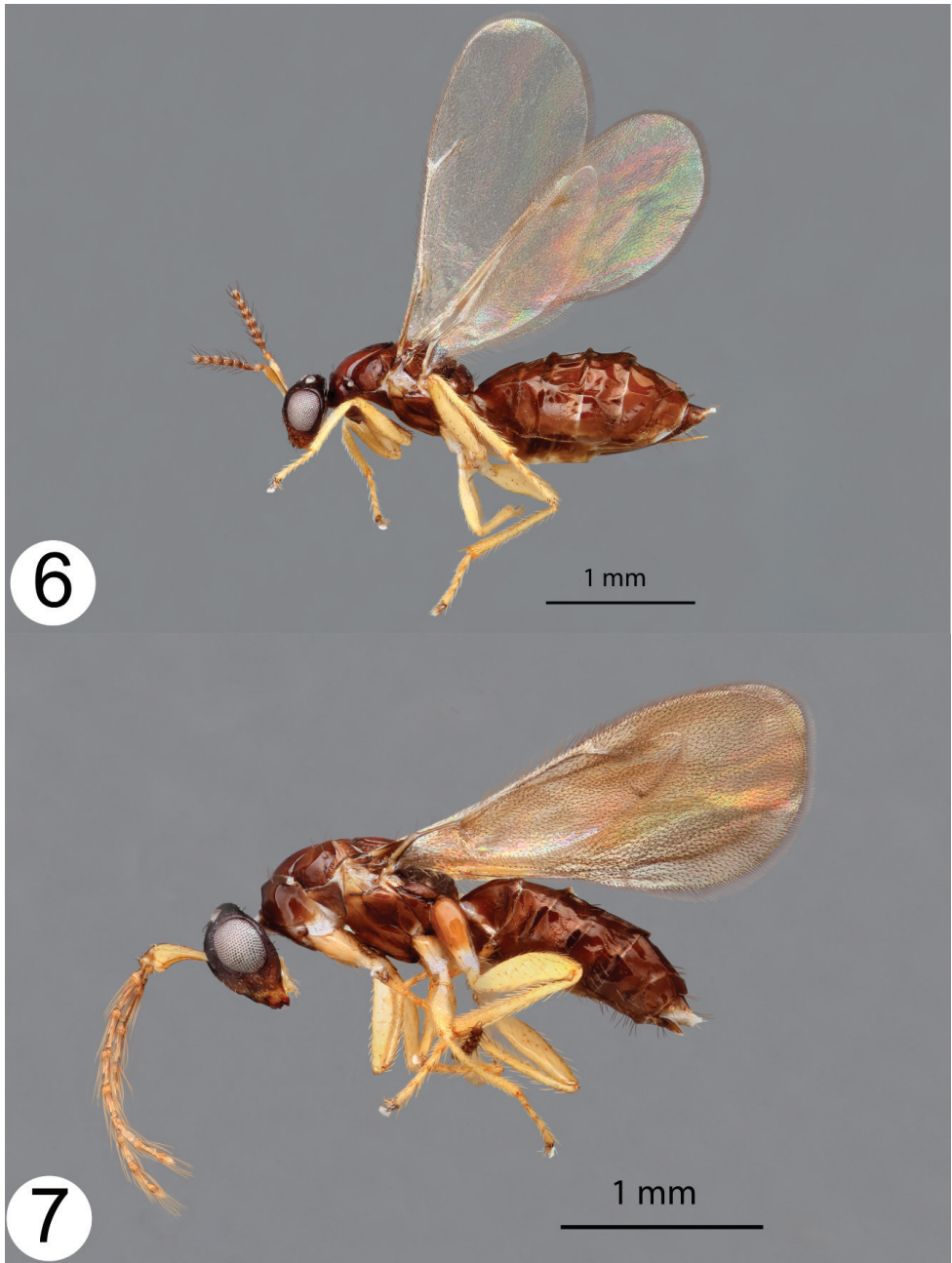


Figure 6–7. Lateral habitus of *Arastichus capipunctata* **6** holotype female **7** paratype male.

Mesosoma. 1.27× as long as broad. Pronotum with two sets of setae postero-laterally. Midlobe of mesoscutum 0.88× as long as broad; smooth, with one pair of adnotaular setae; posterior margin of mesoscutum bilobed (Fig. 24, arrow). Notauli



Figure 8–9. Lateral habitus of *Arastichus gibernau* **8** holotype female **9** paratype male.

complete, shallow. Scutellum 0.90× as long as broad, effaced imbricate, with two pairs of setae; scutellum lacking submedian scutellar grooves, posterior margin rounded. Propodeum raised medially, laterally imbricate, with paraspiracular carina complete.

Prepectus triangular, broadly rounded posteriorly, imbricate. Mesepimeron smooth anteriorly. Epicnemium imbricate. Metapleuron without circular fossa that is at least half as wide as propodeal spiracle. Fore wing with ratio of M:PMV:S as 9:1:4 (Fig. 6); SMV with three setae on dorsal surface.

Metasoma. Finely imbricate; setose along the posterior edges of each gastral tergite; gastral sternites fused or weakly divided; third valvula extends beyond gaster.

Male. Overall morphology and coloration as in female (Fig. 7). Body length 2.9 mm. Antennal ratio of scape (minus radicle):pedicel: A1:F1:F2:F3:F4:F5:F6:club as 25:8:1:2:17:17:17:17:16:9; scape with distinct ventral plaque in apical $\frac{1}{2}$ (Fig. 7), funicular segments clavate basally, with whorl of setae extending $\sim 1.5x$ length of the funicular segment to which it is attached. MPS sparse and located at midlength; clava with basal whorl and apical setae, MPS located at apex (Fig. 7). Genitalia: phallobase less than twice as long as broad, digitus with tooth-like projection on anterior margin, aedeagus broad, with apex rounded (Fig. 27).

Variation. Both sexes: setation and sculpture variable; sometimes with faint traces of submedian scutellar grooves. Females: length of body 2.9–3.2mm, SMV with 2–3 setae. Males: length of body 2.4–2.9mm.

Etymology. Named for the distinctive punctate head.

Biology. Reared from *Philodendron radiatum*.

Distribution. Costa Rica and Mexico.

***Arastichus gallicola* (Ferrière), comb. nov.**

Figs 3–5, 10–20

Trichaporus gallicola, Ferrière, 1924.

Exurus gallicola (Ferrière), Costa Lima (1959)

Aprostocetus gallicola (Ferrière), LaSalle (1994)

Material Examined. **Lectotype** PARAGUAY • [1F, top right of the pin]; 1914, R. Chodat leg., ovaries of *Philodendron selloum* = *Thaumatophyllum bipinnatifidum* (Schott ex Endl.) Sakur., Calazans & Mayo; MNHN. **Paralectotypes** [9F, 4M]; same information as holotype; MNHN. **Other material:** BRAZIL • [37F, 48M]; São Paulo, Ribeirão Preto, University of São Paulo campus, 1.II.2011, Sergio Jansen-González leg., ex galled fruits of *Philodendron bipinnatifidum*; USNM01829346–432; USNM. [11F, 4M] same information; 13.II.2011; MZUSP. [11F, 6M]; São Paulo, Araras Zoo, 14.II.1988, F.D. Bennett leg., *Philodendron* inflorescence; ANIC. [1F]; Nova Tenutonia, 27°11'S, 52°23'W, 300–500m, 12.I.1962, F. Plaumann leg.; CNCI. [1M]; same info as before; V. 1971.; CNCI. [3F]; Rondonia, 62 km SW. Ariquemes near faz. Rancho Grande 26.XII.1992, U. Schmitz leg., blacklight trap; CNCI. [5F] same info as before, J.E. Eger leg., 3–15.XII.1997; CNCI. [3F]; Rondonia, 62 km SW. Ariquemes near faz. Rancho Grande 26.XII.1992, U. Schmitz leg., blacklight trap; CNCI. [5F] same info as before, J.E. Eger leg., 3–15.XII.1997; CNCI. French Guiana • [144F,

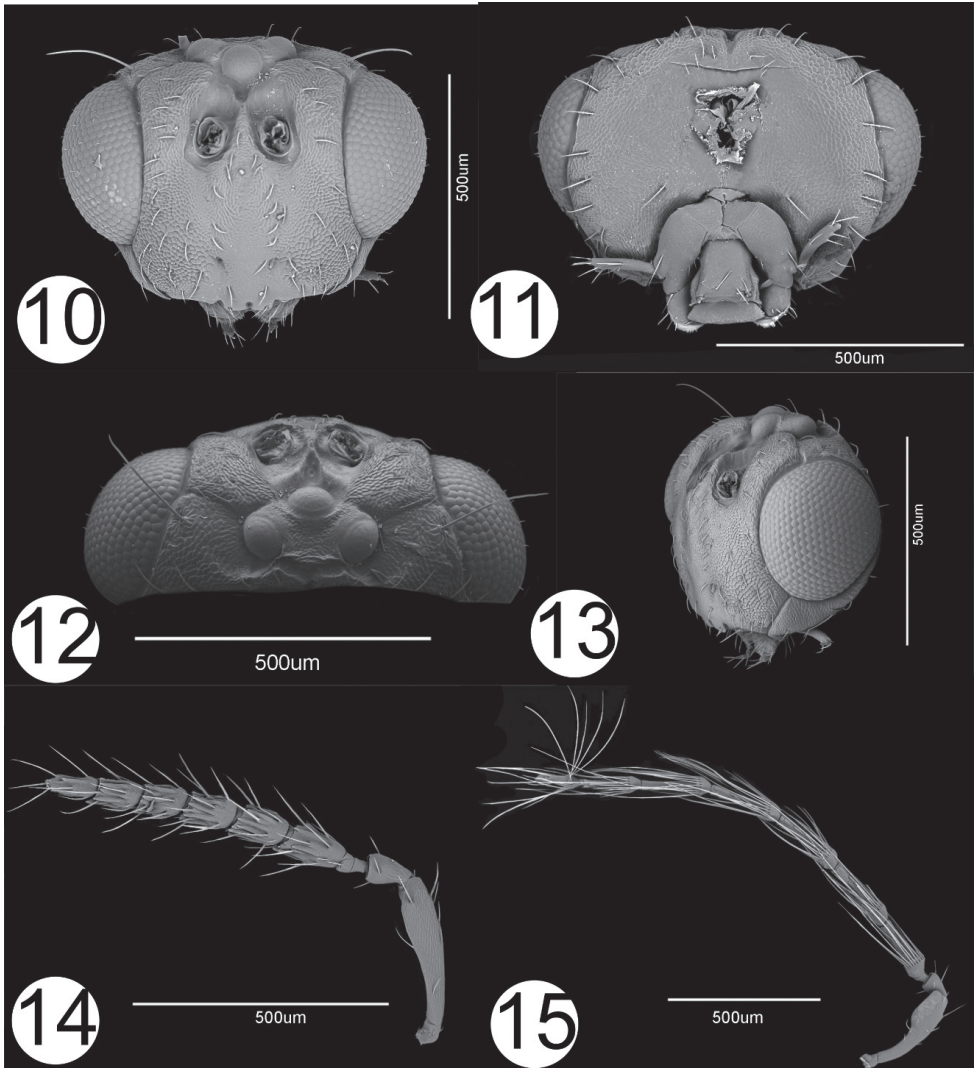


Figure 10–15. *Arastichus gallicola* **10** frontal view of head **11** posterior view of head **12** dorsal view of head **13** anterolateral view of head **14** female antenna **15** male antenna.

54M]; Kourou National Road #1, km 96, 26.IV.2012. M. Gibernau leg. ex. Galled fruits of *Philodendron solimoense*; USNMMENT01829000–01829163; USNM. [4F, 4M] same information as before; ANIC; [4F, 4M] same information as before; BMNH; [4F, 4M] same information as before; CNCI; [4F, 2M] same information as before; CNIN; [4F, 4M] same information as before; MNHN; [9F, 4M] same information as before; MZUCR; [3F] same information as before; MZUSP.

Diagnosis. *Arastichus gallicola* is morphologically similar to *A. gibernau*, but the posterior corner of metapleuron of *A. gallicola* lacks a noticeable fossa, or with an

elongate depression (Fig. 4). Additionally, the vertexal suture is angulate or rounded where it reaches the inner eye margin in *A. gallicola* (Fig. 10), whereas in *A. gibernau* this suture is always rounded.

Description. Female holotype. Body length 3.3 mm. **Color:** Yellow: head, mouthparts, scape, pedicel, mesosoma, femoral depression, acropleuron, legs, ovipositor sheaths; dark brown: funicular segments, apices of mandibles, pronotum immediately surrounding spiracle, scutellum, dorsellum, propodeum, mesopleuron, metapleuron, metasoma. Wing veins white to light brown (Figs 3, 4).

Head. 1.3× as broad as high, effaced imbricate; anterior tentorial pits with epistomal groove extending ventrally (Fig. 10). Supraclypeal area glabrous; clypeus bilobed. Lower margin of eyes slightly sunken; malar suture distinct; malar space 0.58× eye height, asetose beneath eye in elongate microreticulate area; frons protuberant (Fig. 10). Preorbital carina absent; intrascrobal area divergent dorsally to laterad anterior ocellus, delimiting shallow equilateral triangular depression in front of anterior ocellus. Ratio of LOL:OOL:POL as 1:3.1:3.4. Vertexal suture angulate, or rounded at inner eye margin (Fig. 10); occipital margin with transverse, sinuate carina. Head posteriorly lacking postgenal lamina, postgena without ventral depression near ventral margin.

Antenna. (Fig. 14) ratio of scape (minus radicle):pedicel:A1:A2:F1:F2:F3:F4:F5:F6:club as 12.5:3.8:1.3:1:4.5:4.5:4.5:3.8:3.8:5; A1 constricted medially; A2 transverse; two rows of setae on all funicular segments (Fig. 14); erect setae at 45° angle to funicular segment, shorter than the funicular segment to which it is attached to (Fig. 4).

Mesosoma. 1.8× as long as broad. Pronotum with two sets of setae posterolaterally. Midlobe of mesoscutum 1.0× as long as broad; with two pairs of adnotaular setae; posterior margin of mesoscutum not bilobed (Fig. 16). Scutellum 1.2× as long as broad; effaced imbricate, with one to two pairs of setae; notauli complete, shallow; scutellum lacking submedian scutellar grooves, posterior margin rounded. Propodeum raised medially, laterally imbricate, with paraspircular carina complete. Prepectus triangular, broadly rounded posteriorly, imbricate. Mesepimeron striate, becoming smooth anteriorly grading into femoral depression. Epicnemium imbricate. Metapleuron without circular fossa that is at least half as wide as propodeal spiracle. Fore wing with ratio of M:PMV:S as 3:1:1.1 (Fig. 4).

Metasoma. Finely imbricate; setose along the posterior edges of each gastral tergite; gastral sternites fused or weakly divided; third valvula does not extend beyond gaster.

Male. Overall morphology as in female (Fig. 5). Body length 2.5 mm. **Color:** Dark brown except the following golden: base of scape, ventral mouthparts, acropleuron, coxae apically, legs, metatibia in apical 1/4. Antennal ratio of scape (minus radicle):pedicel: A1:F1:F2:F3:F4:F5:F6:club as 6.9:1.4:1:4.3:4.7:4.7:4.3:4.1:3.6:2.9; scape with distinct, white ventral plaque in apical 1/2 (Fig. 5), funicular segments wide at base and narrowing off towards apex, with whorl of setae extending ~1.5× length of the funicular segment to which it is attached, MPS sparse and located at midlength; clava with basal whorl and apical setae, MPS located at apex (Fig. 5). Genitalia: phallobase twice as long as broad, digitus slender without projection on anterior margin, aedeagus slender, with apex pointed; digiti with or without a submedian longitudinal suture from the base of the digital tooth but not reaching the base of the digiti (Fig. 27).

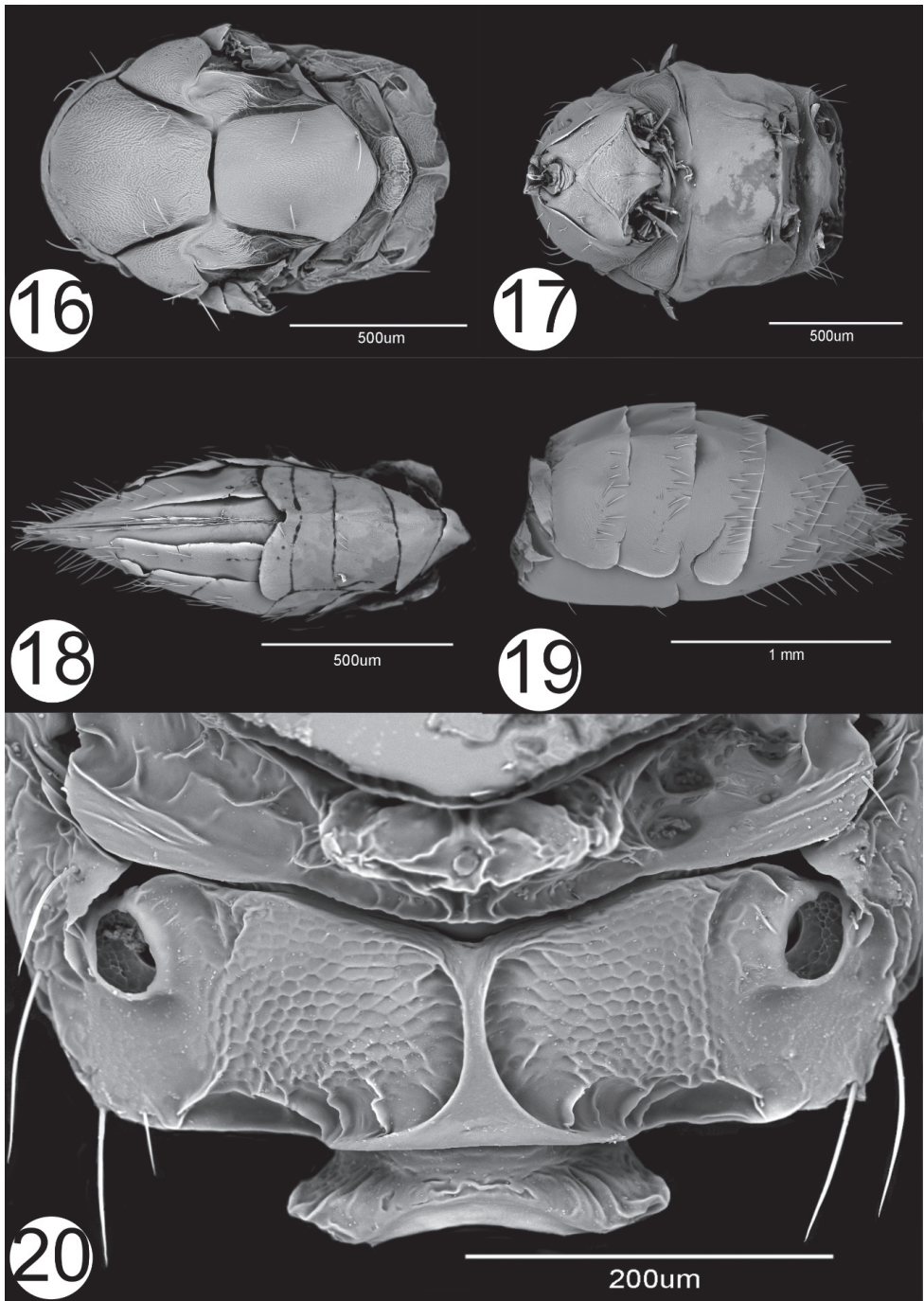


Figure 16–20. *Arastichus gallicola* **16** dorsal view of mesosoma **17** ventral view of mesosoma **18** ventral view of female metasoma **19** lateral view of female metasoma **20** propodeum.

Variation. Both sexes: setation and sculpture variable; sometimes with faint traces of submedian scutellar grooves; vertexal suture can be rounded or angulate. Females: 2.6–3.8mm, scutellum with brown coloration often incomplete laterally, complete medially and anteriorly/posteriorly on scutellar margins; ocellar triangle sometimes brown; pronotal setation ranges from 1–3 per side, adnotaular setation ranges from 1–3 per side with the occasional odd seta in the notaulus; ocellar triangle often with two small divergent setae. Males: 2.5–3.0mm, may have brownish infuscation of the pro- and mesofemur, meso- and metacoxa may be entirely brown. Specimens from Araras Zoo in Brazil consistently had two setae on the lateral lobes of mesoscutum, whereas other specimens had three. However given the lack of other consistent characteristics, we conservatively group them under *A. gallicola*. Variation in female and male genitalia was found. Females reared from *T. bipinnatifidum* showed two distinct ovipositor morphologies with variation due mostly to larger or smaller first and second valvifers. Females reared from *T. solimoense* showed an intermediate size ovipositor. Males reared from *T. solimoense* show a longitudinal submedian suture in the digiti that begins at the base of the digital tooth and does not reach the base of the digiti.

Biology. Reared from *Thaumatophyllum bipinnatifidum* and *T. solimoense*.

Distribution. Brazil and Paraguay.

***Arastichus gibernau* Gates, Hanson, Jansen-González & Zhang, sp. nov.**

<https://zoobank.org/65576A2E-AFA1-4A26-9C76-675B614EAC82>

Figs 8, 9, 24, 25

Material Examined. *Holotype* PANAMA • [1F]; Barro Colorado Island, Canal Zone, 40-22220, J. Zetek leg., ex. *Philodendron oxycardium* flowers, 8.30'40 1.IX.1940 ; USNMMENT01829267; USNM. *Paratypes* [24F, 25M]; same information as holotype; USNMMENT01829268–325; USNM. [3F, 3M]; same information as holotype; ANIC. [4F, 4M]; same information as holotype; BMNH. [4F, 4M]; same information as holotype; CNCI. [4F, 4M]; same information as holotype; MNHN. [4F, 4M]; same information as holotype; MZUCR.

Diagnosis. *Arastichus gibernau* is morphologically similar to *A. gallicola*, but the posterior corner of metapleuron of *A. gibernau* has a noticeable fossa, or with an elongate depression ((Figs 8, 9). Additionally, the vertexal suture is always rounded where it reaches the inner eye margin in *A. gibernau* (Fig. 24), whereas in *A. gallicola* this suture is angulate or rounded (Fig. 10).

Description. Female holotype. Body length 4.4 mm. **Color.** Golden: head, mouthparts, antenna (brownish tint), mesosoma, femoral depression, acropleuron, legs, ovipositor sheaths. Light brown: wing veins, antennae. Dark brown: scutellum, dorsellum, propodeum, metapleuron; wing veins whitish to brownish (Fig. 8).

Head. 1.36× as broad as high, effaced imbricate; anterior tentorial pits with epistomal groove extending ventrally (Fig. 24); supraclypeal area with sparse setae extending from below scrobe to clypeus; clypeus bilobed. Lower margin of eyes slightly sunken;

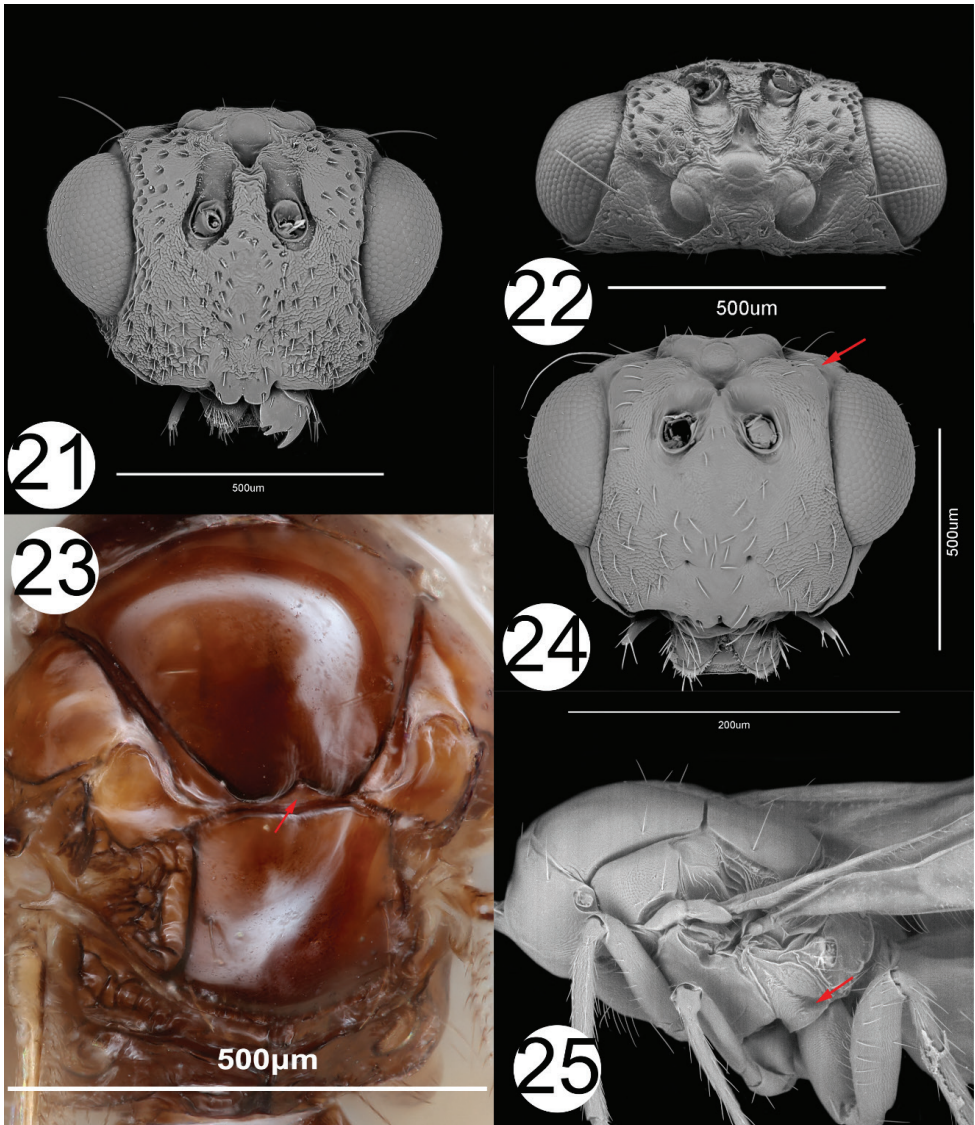


Figure 21–25. *Arastichus capipunctata* **21** frontal view of head **22** dorsal view of head **23** dorsal view of mesosoma, arrow pointing to the bilobed posterior margin of mesoscutum **24–25** *Arastichus gibernau* **24** frontal view of head **25** lateral view of mesosoma, arrow pointing to the circular fossa on the posterior corner of metapleuron.

malar suture distinct; malar space $0.46 \times$ eye height, asetose beneath eye in elongate microreticulate area; frons protubertant. Preorbital carina absent; intrascrobal area divergent dorsally to laterad of anterior ocellus, delimiting shallow, equilateral triangular depression anterad to anterior ocellus. Ratio of LOL:OOL:POL as 1:2.4:2.6. Vertexal suture rounded at inner eye margin (Fig. 24); occipital margin with transverse, sinuate

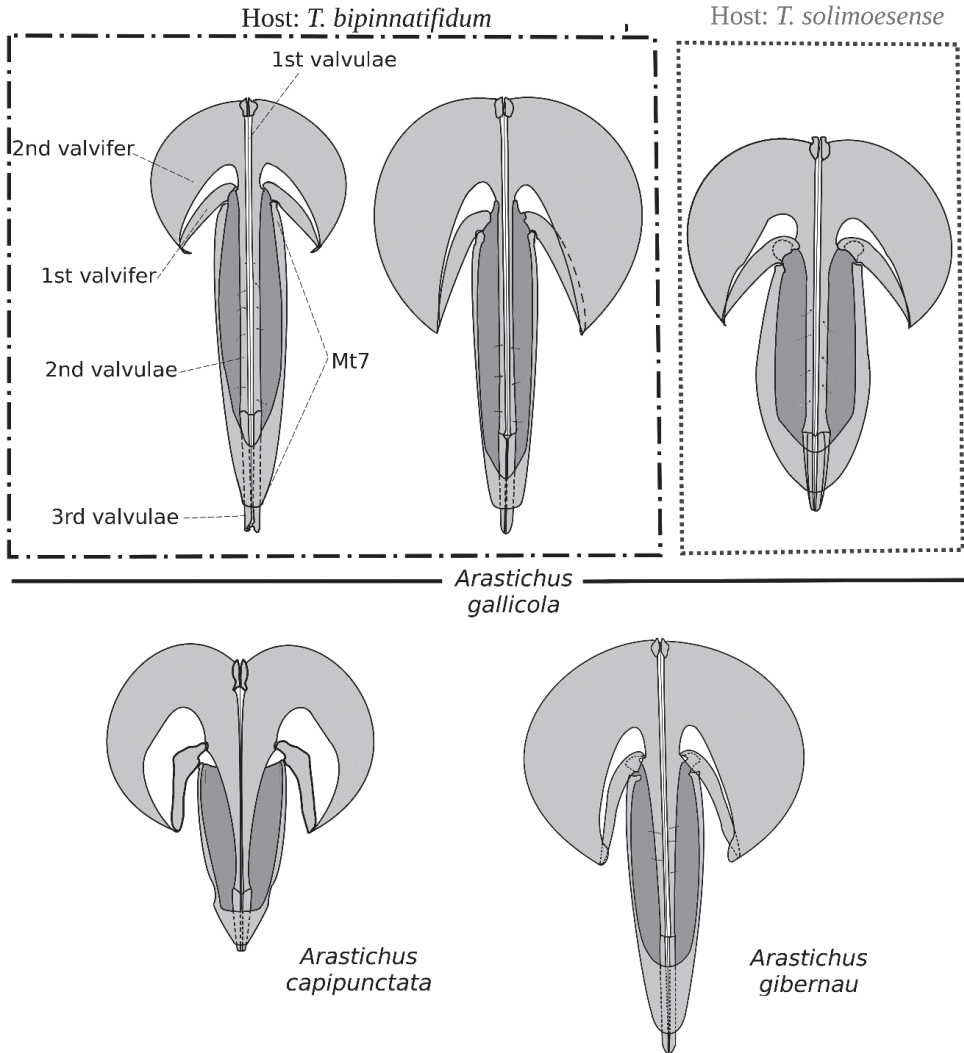


Figure 26. Female genitalia of *Arastichus* spp. based on photographs of slide-mounted specimens. Morphological variations are evident among species and within species.

carina. Head posteriorly lacking postgenal lamina, postgena without ventral depression near ventral margin. Gena expanded ventrally, giving it a “puffy cheeks” appearance.

Antenna. Ratio of scape (minus radicle): pedicel: A1: A2: F1: F2: F3: F4: F5: club as 18:5:1.5:1:8.3:7.3:7:6.3:6.3:2.5 (Fig. 8); A1 constricted medially, A2 transverse, one row of MPS on all funicular segment, two rows of erect setae at 45° angle to funicular segment, shorter than the funicular segment to which it is attached (Fig. 8).

Mesosoma. 1.34× as long as broad. Pronotum with three sets of setae posterolaterally. Midlobe of mesoscutum 0.73× as long as broad; with two pairs of adnotaular

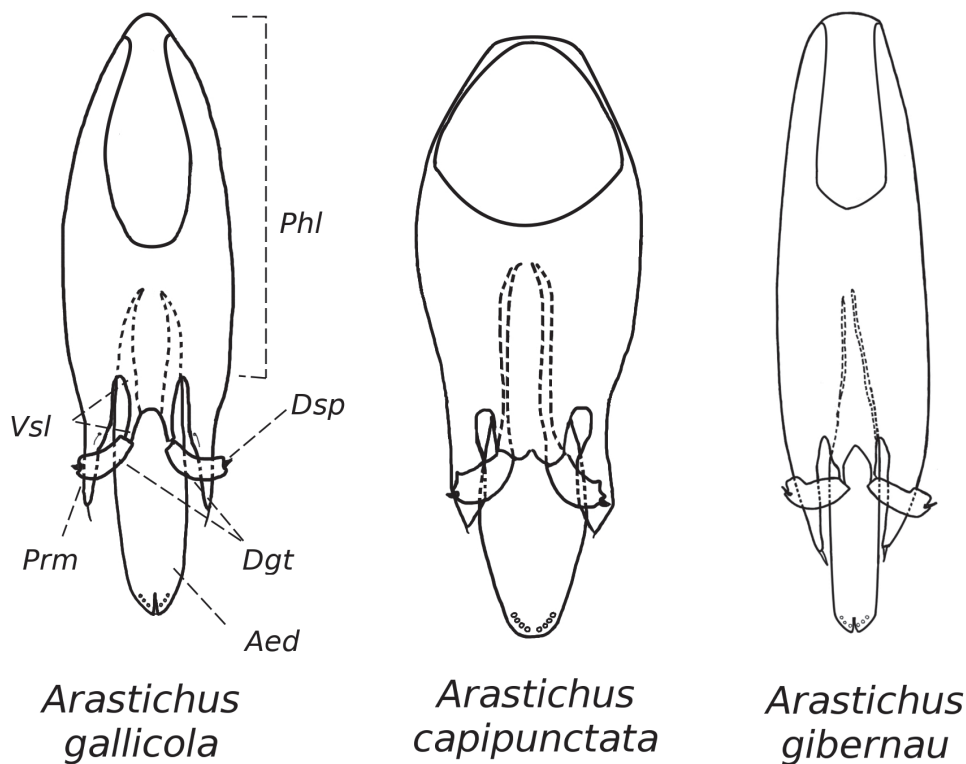


Figure 27. Male genitalia of *Arastichus* spp. based on photographs of slide-mounted specimens. *Dsp* digital spine; *Aed* aedeagus; *Dgt* digitus; *Dsp* digital spine; *Phl* phallobase; *Prm* paramere; *Vsl* volsella.

setae; posterior margin of mesoscutum not bilobed. Notauli complete, shallow. Scutellum 1.01x as long as broad; effaced imbricate, with two pairs of setae. Metapleuron with circular fossa that is at least half as wide as propodeal spiracle (Figs 8, 25 arrow). Propodeum raised medially, laterally imbricate, with paraspiracular carina complete. Prepectus triangular, broadly rounded posteriorly, imbricate. Mesepimeron striate, becoming smooth anteriorly grading into femoral depression. Epicnemium imbricate. Fore wing with ratio of M:PMV:S as 2.5:3.3:1.

Metasoma. Finely imbricate (Fig. 8); setose along the posterior edges of each gastral tergite; third valvula extends beyond metasoma.

Male. Overall morphology as in females (Fig. 9). Body length 3.3 mm. **Color:** Dark brown except the following white: all tibia, procoxa apically, pro- and meso femur, metatibia in apical 1/4. Antennal ratio of scape (minus radicle):pedicel: A1:F1:F2:F3:F4:F5:F6:club as 10.3:2.5:1:6.8:6.8:6.8:6.5:5.3:4.8:3.5; scape with distinct ventral plaque in apical 1/2 (Fig. 9), funicular segments clavate basally, with whorl of setae extending ~1.5x length of the funicular segment to which it is attached, MPS sparse and located at midlength; clava with basal whorl and apical setae, MPS located at apex (Fig. 9). Genitalia: phallobase twice as long as broad, digitus slender with a blunt projection on anterior margin, aedeagus slender, with apex pointed (Fig. 27).

Variation. Considerable variation is noted. Females: 3.5–5.2mm, pronotal setation ranges from 1–3 per side, adnotaular setation ranges from 1–2 per side. Males: 2.8–3.5mm, may have brownish infuscation of the pro- and mesofemur.

Etymology. Named in honor of Dr. Marc Gibernau for providing a very large sample of specimens of this species for our research.

Biology. Reared from *Philodendron hederaceum* var. *oxycardium*.

Distribution. Panama.

Discussion

Gall induction have evolved multiple times within Tetrastichinae, and to date is known from 10 different host plant families (LaSalle 1994; Fisher et al. 2014; Gates et al. 2020; Singh et al 2022) around the world. However, given the diversity and the lack of taxonomic attention in recent years, the true number of tetrastichine gall inducers is likely much higher. Hopefully with the advances of phylogenomic techniques such as UCEs and broader taxonomic sampling of species-rich regions such as the Neotropics, we can gain a better understanding of the true diversity of gall induction within Eulophidae and Chalcidoidea as a whole.

Acknowledgements

We thank Barry Hammel of the Missouri Botanical Gardens and Christian Trejos of the University of Costa Rica for helping with plant identifications in Costa Rica, and Taina Litwak of USDA SEL for the illustration. We thank Christer Hansson and one anonymous reviewer for providing valuable feedback that have improved the manuscript. SJG was supported by FAPESP (#09/10273-9). The computations in this paper were conducted on the Smithsonian High Performance Cluster (SI/HPC), Smithsonian Institution. <https://doi.org/10.25572/SIHPC>. YMZ is supported by Oak Ridge Institute for Science and Education (ORISE) fellowship. Mention of trade names or commercial products in this publication is solely for the purpose of providing specific information and does not imply recommendation or endorsement by the USDA. USDA is an equal opportunity provider and employer.

References

Bankevich A, Nurk S, Antipov D, Gurevich AA, Dvorkin M, Kulikov AS, Lesin VM, Nikolenko SI, Pham S, Pribelski AD, Pyshkin AV, Sirotkin AV, Vyahhi N, Tesler G, Alekseyev MA, Pevzner PA (2012) SPAdes: a new genome assembly algorithm and its applications to single-cell sequencing. *Journal of Computational Biology* 19: 455–477. <https://doi.org/10.1089/cmb.2012.0021>

- Branstetter MG, Longino JT, Ward PS, Faircloth BC, Price S (2017) Enriching the ant tree of life: enhanced UCE bait set for genome-scale phylogenetics of ants and other Hymenoptera. *Methods in Ecology and Evolution* 8: 768–776. <https://doi.org/10.1111/2041-210X.12742>
- Böhmová J, Rasplus J-Y, Taylor GS, Janšta P (2022) Description of two new Australian genera of Megastigmidae (Hymenoptera, Chalcidoidea) with notes on the biology of the genus *Bortesia*. *Journal of Hymenoptera Research* 90: 75–99. <https://doi.org/10.3897/jhr.90.82582>
- Buffington M, Burks R, McNeil L (2005) Advanced techniques for imaging parasitic Hymenoptera (Insecta). *American Entomologist* 51: 50–56. <https://doi.org/10.1093/ae/51.1.50>
- Buffington ML, Gates MW (2008) Advanced imaging techniques II: using a compound microscope for photographing point-mount specimens. *American Entomologist* 54: 222–224. <https://doi.org/10.1093/ae/54.4.222>
- Burks BD (1971) A synopsis of the genera of the family Eurytomidae (Hym., Chalcidoidea). *Transactions of the American Entomological Society* 97(1): 1–89.
- Castresana J (2000) Selection of conserved blocks from multiple alignments for their use in phylogenetic analysis. *Molecular Biology and Evolution*: 17(4): 540–552. <https://doi.org/10.1093/oxfordjournals.molbev.a026334>
- Costa Lima A da (1959a) *Trichaporus*, *Trichoporos* ou *Exurus*? (Hym. Chalcidoidea, Eulophidae, Tetrastichinae). *Anais da Academia Brasileira de Ciências* 31(1): 119–128.
- Costa Lima A da (1959b) Duas novas espécies de *Exurus* da Bahia (Hym. Chalcidoidea, Eulophidae, Tetrastichinae). *Anais da Academia Brasileira de Ciências* 31(1): 129–133.
- Cruaud A, Nidelet S, Arnal P, Weber A, Fusu L, Gumovsky A, Huber J, Polaszek A, Rasplus J-Y (2019) Optimized DNA extraction and library preparation for minute arthropods: application to target enrichment in chalcid wasps used for biocontrol. *Molecular Ecology Resources* 19(3): 702–710. <https://doi.org/10.1111/1755-0998.13006>
- De Santis L (1979) Catálogo de los himenópteros calcidoideos de América al sur de los Estados Unidos. *Publicación Especial Comisión de Investigaciones Científicas Provincia de Buenos Aires*, 82 pp.
- De Santis L (1980) *Catálogo de los Himenópteros Brasileños de la serie Parasítica incluyendo Bethyloidea*. Editora da Universidade Federal do Paraná, Curitiba, 395 pp.
- De Santis L, Fidalgo P (1994) *Catálogo de Himenópteros Calcidoideos*. Serie de la Academia Nacional de Agronomía y Veterinaria No 13: 1–145.
- Faircloth BC, McCormack JE, Crawford NG, Harvey MG, Brumfield RT, Glenn TC (2012) Ultraconserved elements anchor thousands of genetic markers spanning multiple evolutionary timescales. *Systematic Biology* 61(5): 717–726. <https://doi.org/10.1093/sysbio/sys004>
- Faircloth BC (2016) PHYLUCE is a software package for the analysis of conserved genomic loci. *Bioinformatics* 32(5): 786–788. <https://doi.org/10.1093/bioinformatics/btv646>
- Ferrière C (1924) Note sur deux nouveaux Chalcidiens phytophages du Paraguay. *Annales de la Société Entomologique de France* 93: 1–21.
- Fisher N, Moore A, Brown B, Purcell M, Taylor GS, LaSalle J (2014) Two new species of *Selitrichodes* (Hymenoptera: Eulophidae: Tetrastichinae) inducing galls on Casuarina (Casuarinaceae). *Zootaxa* 3790: 534–542. <https://doi.org/10.11646/zootaxa.3790.4.2>

- Gates MW, Zhang YM, Buffington ML (2020) The great greenbriers gall mystery resolved? New species of *Aprostocetus* Westwood (Hymenoptera, Eulophidae) gall inducer and two new parasitoids (Hymenoptera, Eurytomidae) associated with *Smilax* L. in southern Florida, USA. *Journal of Hymenoptera Research* 80: 71–98. <https://doi.org/10.3897/jhr.80.59466>
- Gibernau M, Albre J, DeJean A, Barabet D (2002) Seed predation in *Philodendron solimoesense* (Araceae) by chalcid wasps (Hymenoptera). *International Journal of Plant Science* 163: 1017–1023. <https://doi.org/10.1086/342628>
- Gibson GAP (1997) Morphology and terminology. In: Gibson GA, Huber JT, Woolley JB (Eds) *Annotated keys to the genera of Nearctic Chalcidoidea* (Hymenoptera). NRC Research Press, Ottawa, ON, 16–44.
- Guindon S, Dufayard JF, Lefort V, Anisimova M, Hordijk W, Gascuel O (2010) New algorithms and methods to estimate maximum-likelihood phylogenies: assessing the performance of PhyML 3.0. *Systematic Biology* 59(3): 307–321. <https://doi.org/10.1093/sysbio/syq010>
- Hansson C (2004) Eulophidae of Costa Rica (Hymenoptera: Chalcidoidea), 2. *Memoirs of the American Entomological Institute* 75: 536 pp.
- Harris RA (1979) Glossary of surface sculpturing. *Occasional Papers in Entomology* 28: 1–31.
- Heraty J, Hawks D (1998) Hexamethyldisilazane – a chemical alternative for drying insects. *Entomological News* 109: 369–374.
- Heraty JM, Burks RA, Cruaud A, Gibson, GAP, Liljebblad J, Munro M, Rasplus J-Y, Delvare G, Janšta P, Gumovsky A, Huber J, Woolley JB, Krogmann L, Heydon S, Polaszek A, Schmidt S, Darling DC, Gates MW, Mottern J, Murray E, Molin AD, Triapitsyn S, Baur H, Pinto JD, van Noort S, George J, Yoder M (2013) A phylogenetic analysis of the megadiverse Chalcidoidea (Hymenoptera). *Cladistics* 29(5): 466–542. <https://doi.org/10.1111/cla.12006>
- Hoang DT, Chernomor O, Von Haeseler A, Minh BQ, Vinh LS (2018) UFBoot2: improving the ultrafast bootstrap approximation. *Molecular Biology and Evolution* 5(2): 518–522. <https://doi.org/10.1093/molbev/msx281>
- Infante F, Hanson PE, Wharton RA (1995) Phytophagy in the genus *Monitoriella* (Hymenoptera: Braconidae) with description of new species. *Annals of the Entomological Society of America* 88(4): 406–415. <https://doi.org/10.1093/aesa/88.4.406>
- Kalyaanamoorthy S, Minh BQ, Wong TK, Von Haeseler A, Jermiin LS (2017) ModelFinder: fast model selection for accurate phylogenetic estimates. *Nature Methods* 14(6): 587–589. <https://doi.org/10.1038/nmeth.4285>
- Katoh K, Toh H (2008) Recent developments in the MAFFT multiple sequence alignment program. *Briefings in Bioinformatics* 9(4): 286–298. <https://doi.org/10.1093/bib/bbn013>
- Kerr PH, Fisher EM, Buffington ML (2008) Dome lighting for insect imaging under a microscope. *American Entomologist* 54: 198–200. <https://doi.org/10.1093/ae/54.4.198>
- Kim I-K, Delvare G, LaSalle J (2004) A new species of *Quadrastichus* (Hymenoptera: Eulophidae): a gall-inducing pest on *Erythrina* (Fabaceae). *Journal of Hymenoptera Research* 13: 243–249.
- Kim I-K, LaSalle J (2008) A new genus and species of Tetrastichinae (Hymenoptera: Eulophidae) inducing galls in seed capsules of *Eucalyptus*. *Zootaxa* 1745: 63–68. <https://doi.org/10.11646/zootaxa.1745.1.6>

- Kim I-K, McDonald M, LaSalle J (2005) *Moona*, a new genus of tetrastichine gall inducers (Hymenoptera: Eulophidae) on seeds of *Corymbia* (Myrtaceae) in Australia. *Zootaxa* 989: 1–10. <https://doi.org/10.11646/zootaxa.989.1.1>
- LaSalle J (1994) North American genera of Tetrastichinae (Hymenoptera: Eulophidae). *Journal of Natural History* 28: 109–236. <https://doi.org/10.1080/00222939400770091>
- LaSalle J (2005) Biology of gall inducers and evolution of gall induction in Chalcidoidea (Hymenoptera: Eulophidae, Eurytomidae, Pteromalidae, Tanaostigmatidae, Torymidae). In: Raman A, Schaefer CW, Withers TM (Eds) *Biology, Ecology, and Evolution of Gall-inducing Arthropods*. Science Publishers, Inc., Enfield, NH, 509–537.
- Lotfalizadeh H, Delvare G, Rasplus J-Y (2007) Phylogenetic analysis of Eurytominae (Chalcidoidea: Eurytomidae) based on morphological characters. *Zoological Journal of the Linnean Society* 151: 441–510. <https://doi.org/10.1111/j.1096-3642.2007.00308.x>
- Mayo, SJ (1991) A Revision of *Philodendron* Subgenus *Meconostigma* (Araceae) *Kew Bulletin* 46: 601–681. <https://doi.org/10.2307/4110410>
- Mendel Z, Protasov A, Fisher N, LaSalle J (2004) Taxonomy and biology of *Leptocybe invasa* gen. & sp. n. (Hymenoptera: Eulophidae), an invasive gall inducer on *Eucalyptus*. *Australian Journal of Entomology* 43: 101–113. <https://doi.org/10.1111/j.1440-6055.2003.00393.x>
- Minh BQ, Schmidt HA, Chernomor O, Schrempf D, Woodhams MD, Von Haeseler A, Lanfear R (2020) IQ-TREE 2: new models and efficient methods for phylogenetic inference in the genomic era. *Molecular Biology and Evolution*. 37(5): 1530–1534. <https://doi.org/10.1093/molbev/msaa015>
- Noyes JS (2019) Universal Chalcidoidea Database. www.nhm.ac.uk/entomology/Chalcidooids/index.html [accessed on 21 Dec 2021]
- Perioto NW, Lara RIR (2019) New distributional record of *Prodecatoma philodendri* Ferrière (Hymenoptera: Eurytomidae), with a checklist of *Prodecatoma* Ashmead species and new host plant family for the genus. *Revista Chilena de Entomología*: 45(3): 463–469.
- Rasplus J-Y, LaSalle J, Delvare G, Mckey D, Webber BL (2011) A new Afrotropical genus and species of Tetrastichinae (Hymenoptera: Eulophidae) inducing galls on *Bikinia* (Fabaceae: Caesalpinioideae) and a new species of *Ormyrus* (Hymenoptera: Ormyridae) associated with the gall. *Zootaxa* 2907: 51–59.
- Rasplus J-Y, Blaimer BB, Brady SG, Burks RA, Delvare G, Fisher N, Gates M, Gauthier NA, Gumovsky AV, Hansson C, Heraty JM, Fusu L, Nideler S, Pereira RAS, Sauné L, Ubaidillah R, Cruaud A (2020) A first phylogenomic hypothesis for Eulophidae (Hymenoptera, Chalcidoidea). *Journal of Natural History* 54: 597–609. <https://doi.org/10.1080/00222933.2020.1762941>
- Sakuragui CM, Calazans LSB, de Oliveira LL, de Moraes EB, Benko-Iseppon AM, Vasconcelos S, Schrago CEG, Joseph Mayo SJ (2018) Recognition of the genus *Thaumatophylum* Schott – formerly *Philodendron* subg. *Meconostigma* (Araceae) – based on molecular and morphological evidence. *PhytoKeys* 98: 51–71. <https://doi.org/10.3897/phytokeys.98.25044>
- Shimbori EM, Penteado-Dias AM, Nunes JF (2011) *Monitoriella* Hedqvist (Hymenoptera: Braconidae: Doryctinae) from Brazil, with descriptions of three new species. *Zootaxa* 2921: 28–38. <https://doi.org/10.11646/zootaxa.2921.1.3>

Singh S, Kumar A, Kaneria M (2022) Description of five new eulophid species (Hymenoptera: Eulophidae) associated with leaf vein galls of *Madhuca longifolia* (J. Koenig) (Sapotaceae) in India. *Zootaxa* 5129: 1–36. <https://doi.org/10.11646/zootaxa.5129.1.1>

Supplementary material I

Table S1

Authors: Y. Miles Zhang, Michael W. Gates, Paul E. Hanson, Sergio Jansen-González
Data type: Specimen information.

Explanation note: Locality information and accession numbers for UCE/Sanger loci.

Copyright notice: This dataset is made available under the Open Database License (<http://opendatacommons.org/licenses/odbl/1.0/>). The Open Database License (ODbL) is a license agreement intended to allow users to freely share, modify, and use this Dataset while maintaining this same freedom for others, provided that the original source and author(s) are credited.

Link: <https://doi.org/10.3897/jhr.92.85967.suppl1>